

Reversible Photoswitching of Ferromagnetic FePt Nanoparticles at Room Temperature

Masayuki Suda,[†] Masaru Nakagawa,[‡] Tomokazu Iyoda,[‡] and Yasuaki Einaga^{*†}

Contribution from the Department of Chemistry, Faculty of Science and Technology, Keio University, 3-14-1 Hiyoshi, Yokohama 223-8522, Japan, and Chemical Resources Laboratory, Tokyo Institute of Technology, 4259 Nagatsuta, Yokohama 226-8503, Japan

Received November 23, 2006; E-mail: einaga@chem.keio.ac.jp

Abstract: There has been a great interest in developing photoswitchable magnetic materials because of their possible applications for future high-density information storage media. In fact, however, the examples reported so far did not show ferromagnetic behavior at room temperature. From the viewpoint of their practical application to magnetic recording systems, the ability to fix their magnetic moments such that they still exhibit room-temperature ferromagnetism is an absolute requirement. Here, we have designed reversible photoswitchable ferromagnetic FePt nanoparticles whose surfaces were coated with azobenzene-derivatized ligands. On the surfaces of core particles, reversible photoisomerization of azobenzene in the solid state was realized by using spacer ligands that provide sufficient free volume. These photoisomerizations brought about changes in the electrostatic field around the core-FePt nanoparticles. As a result, we have succeeded in controlling the magnetic properties of these ferromagnetic composite nanoparticles by alternating the photoillumination in the solid state at room temperature.

Introduction

Optically switchable magnetic materials have recently been attracting great interest because of the continuing demand for the development of future optical memory.^{1,2} However, the only observations of such optical switching that have been reported so far have been limited to very low-temperature operation. To realize practical optical switching at room temperature, we have proposed a novel strategy that involves the incorporation of organic photochromes into an inorganic magnetic system on a nanometer-scale order. The photochromes not only change their adsorption spectra, they also change their physical and chemical properties, meaning that the magnetic properties of such composite materials can be controlled by photoillumination. Indeed, on the basis of this idea, we have already reported some optically switchable magnetic materials.³ Although the examples described above exhibit photoswitching even at room temperature,^{3c,e} these systems still also show

superparamagnetic behavior at room temperature. This is because decreases in particle size lead to thermal fluctuations in magnetization, resulting in the disappearance of ferromagnetism. From the viewpoint of their practical application to magnetic recording systems, the ability to fix their magnetic moments such that they still exhibit room-temperature ferromagnetism is an absolute requirement.

Here, we focused on L1₀ FePt alloys (also known in the fct phase) for the inorganic magnetic system. These L1₀ FePt nanoparticles are promising materials for future high-density magnetic recording media due to their uniaxial magnetocrystalline anisotropy ($K_u = 7 \times 10^6 \text{ J m}^{-3}$)⁴ and excellent chemical stability. Moreover, chemically synthesized FePt nanoparticles have recently attracted much attention due to their narrow size distribution (with a few nanometer scale)⁵ as compared to those fabricated by existing sputtering techniques. However, these methods usually require a subsequent thermal annealing process to produce structural transitions to the ordered L1₀ phase.

In this study, we have focused on the direct synthesis of the fct phase, which is the so-called “polyol process”,⁶ with the

[†] Keio University.

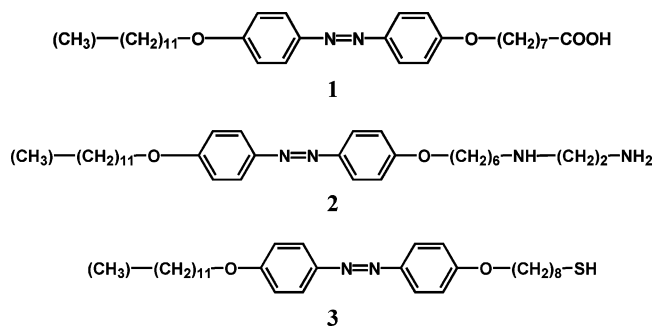
[‡] Tokyo Institute of Technology.

- (1) (a) Kuhl, W. *Nat. Mater.* **2003**, *2*, 505. (b) Thirion, C.; Wernsdorfer, W.; Mailly, D. *Nat. Mater.* **2003**, *2*, 524. (c) Matsuda, K.; Irie, M. *J. Am. Chem. Soc.* **2000**, *122*, 7195. (d) Gütlich, P.; Garcia, Y.; Woike, T. *Coord. Chem. Rev.* **2001**, *219*, 839.
- (2) (a) Sato, O.; Iyoda, T.; Fujishima, A.; Hashimoto, K. *Science* **1996**, *272*, 704. (b) Sato, O.; Einaga, Y.; Iyoda, T.; Fujishima, A.; Hashimoto, K. *J. Electrochem. Soc.* **1997**, *144*, L11. (c) Yamamoto, Y.; Umemura, Y.; Sato, O.; Einaga, Y. *J. Am. Chem. Soc.* **2005**, *127*, 16065. (d) Taguchi, M.; Yagi, I.; Nakagawa, M.; Iyoda, T.; Einaga, Y. *J. Am. Chem. Soc.* **2006**, *128*, 10978.
- (3) (a) Einaga, Y.; Sato, O.; Iyoda, T.; Fujishima, A.; Hashimoto, K. *J. Am. Chem. Soc.* **1999**, *121*, 3745. (b) Yamamoto, T.; Umemura, Y.; Sato, O.; Einaga, Y. *Chem. Mater.* **2004**, *16*, 1195. (c) Mikami, R.; Taguchi, M.; Yamada, K.; Suzuki, K.; Sato, O.; Einaga, Y. *Angew. Chem., Int. Ed.* **2004**, *43*, 6135. (d) Taguchi, M.; Yamada, K.; Suzuki, S.; Sato, O.; Einaga, Y. *Chem. Mater.* **2005**, *17*, 4554. (e) Suda, M.; Miyazaki, Y.; Hagiwara, Y.; Sato, O.; Shiratori, S.; Einaga, Y. *Chem. Lett.* **2005**, *34*, 7, 1028.

- (4) Ivanov, O. A.; Solina, L. V.; Demeshina, V. A.; Magat, L. M. *Phys. Met. Metallogr.* **1973**, *35*, 81.
- (5) (a) Sun, S.; Murray, C. B.; Weller, D.; Folks, L.; Moser, A. *Science* **2000**, *287*, 1989. (b) Elkins, K. E.; Vedantam, T. S.; Liu, J. P.; Zeng, H.; Sun, S.; Ding, Y.; Wang, Z. L. *Nano Lett.* **2003**, *3*, 1647. (c) Chen, M.; Kim, J.; Liu, J. P.; Fan, H.; Sun, S. *J. Am. Chem. Soc.* **2006**, *128*, 7132. (d) Sun, S.; Anders, S.; Thomson, T.; Baglin, J. E. E.; Toney, M. F.; Hamann, H. F.; Murray, C. B.; Terris, B. D. *J. Phys. Chem. B* **2003**, *107*, 5419.
- (6) (a) Sato, K.; Jeyadevan, B.; Tohji, K. *J. Magn. Magn. Mater.* **2005**, *289*, 1. (b) Teng, X.; Yang, H. *J. Am. Chem. Soc.* **2003**, *125*, 14559. (c) Minami, R.; Kitamoto, Y.; Chikata, T.; Kato, S. *Electrochim. Acta* **2005**, *51*, 864. (d) Sort, J.; Surinach, S.; Baro, M. D.; Muraviev, D.; Dzhardimalieva, G. I.; Golubeva, N. D.; Pomogalio, S. I.; Pomogalio, A. D.; Macedo, W. A. A.; Weller, D.; Skumryev, V.; Nogues, J. *Adv. Mater.* **2006**, *18*, 4.

aim of achieving surface modification by the application of photofunctional ligands. The advantages of these direct syntheses techniques are that they prevent particle aggregation during the annealing process and they enable the possibility for surface modification by using functional organic ligands. In the field of nanosized metallic particles, surface modification is a useful method for functionalizing the properties of the material, because the surface plays a crucial role in determining the electronic properties of the particles as a whole.⁷ In fact, our previous works have shown that magnetic nanoparticles whose surfaces are coated by photochromes can exhibit reversible photoswitching of magnetization.^{3c,e}

In the current system, we have designed several types of ferromagnetic FePt nanoparticles coated with azobenzene-derivatized ligands, such as compounds **1** (8-[4-(4-dodecyloxy-phenylazo)-phenoxy]-octanoic acid), **2** (*N*¹-{6-[4-(4-dodecyloxy-phenylazo)-phenoxy]-hexyl}-ethane-1,2-diamine), and **3** (8-[4-(4-dodecyloxy-phenylazo)-phenoxy]-octane-1-thiol). In addition to azobenzene-derivatized ligands, we have also used *n*-octylamine or octanoic acid as “spacer ligands”. These “spacer ligands” enable the reversible photoisomerization of azo-ligands, even in the solid state. Further details about this will be discussed later. As a result, these composite nanoparticles showed ferromagnetic behavior, and their magnetic properties were reversibly controllable by photoillumination, even at room temperature.



Experimental Section

Synthesis. Azo-ligands **1**,^{8,9} and **3**¹⁰ and FePt nanoparticles^{6a} were synthesized in a manner similar to methods described in the literature.

The composite FePt nanoparticles were prepared as follows: Stoichiometric azo-ligands **1** and *n*-octylamine (or azo-ligands **2**) dissolved in warm toluene were added to as-synthesized FePt nanoparticles dispersed in tetraethylene glycol. Next, the mixture was stirred vigorously at 100 °C under an N₂ atmosphere. After several hours, the toluene phase turned from yellow to dark brown, indicating the presence of ligand-coated nanoparticles in the toluene phase. After being cooled to room temperature, the toluene phase was separated, and then an excess amount of ethanol was added to precipitate the nanoparticles. The black precipitate was separated by centrifugation (6000 rpm, 10 min). The black product was redispersed in ethanol and separated by centrifugation again. This washing process was repeated several times to remove excess organic ligands and then dried in air.

Another set of composite nanoparticles stabilized with azo-ligands **3** was prepared as follows: The FePt nanoparticles were dispersed in

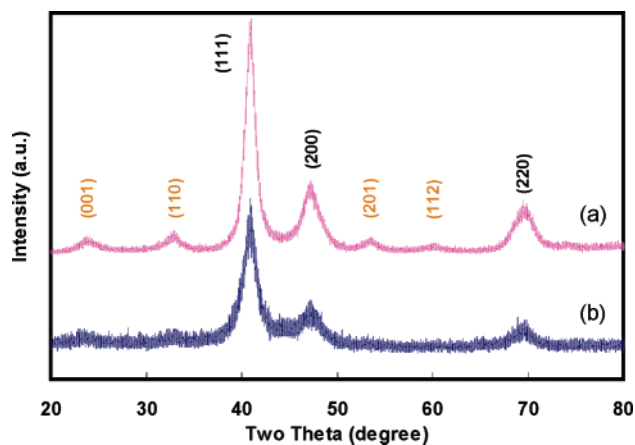


Figure 1. XRD pattern for the FePt nanoparticles. (a) XRD pattern of the as-prepared state. The weak peaks for (001), (110), (201), and (112) are typical superlattice reflections that indicate the existence of the partially ordered L1₀ phase in the synthesized FePt nanoparticles. (b) XRD pattern of the composite state. Superlattice reflections such as (001) and (110) are still observed for the composite state, meaning that the partially ordered L1₀ phase was maintained even after surface modification.

hexane following the same method as described above by using octanoic acid and octylamine as the ligands. Next, the octylamine was exchanged with azo-ligands **3** in dichloromethane by means of a ligand exchange method.¹¹

Physical Methods. The UV/vis spectra were recorded on a V-560 spectrometer (JASCO). UV illumination (filtered light, $\lambda_{\text{max}} = 360$ nm, 1.0 mW cm⁻²) was applied with an ultrahigh-pressure mercury lamp (HYPERCURE 200, Yamashita Denso). Visible light (400–700 nm, 1.0 mW cm⁻²) was provided by a xenon lamp (XFL-300, Yamashita Denso). The magnetic properties were investigated with a SQUID magnetometer (model MPMS-XL Quantum Design). The lamps were guided into the SQUID magnetometer by an optical fiber to study the photomagnetic effects. ⁵⁷Fe Mössbauer spectra were measured with a Topologic Systems model 222 constant-acceleration spectrometer with a ⁵⁷Co/Rh source in transmission mode. The XPS spectra were obtained on a JPS-9000MC (JEOL) using the Al K α line source. The X-ray diffraction patterns were recorded on a RAD-C (RIGAKU) using Ni-filtered Cu K α radiation.

Results and Discussion

Characterization of Composite Nanoparticles. Figure 1 shows the powder XRD pattern of the FePt nanoparticles in as-prepared and composite states. The weak peaks for (001), (110), (201), and (112) in the as-prepared state are typical superlattice reflections that cannot be observed in the disordered fcc phase. These superlattice reflections suggest the existence of the partially ordered L1₀ phase in the synthesized FePt nanoparticles. It has been reported that the phase transition temperature (*T*_t) of the FePt nanoparticles is reduced to about 300 °C when using ethylene glycol as the solvent, whereas tetraethylene glycol (TEG) has a boiling point of 327 °C, which is higher than *T*_t.^{6a} Therefore, carrying out the synthesis above 300 °C made the phase transition from the disordered fcc phase to the partially ordered L1₀ phase possible for the synthesized FePt nanoparticles. The XRD pattern of the composite nanoparticles also shows superlattice reflections that indicate that partially ordered L1₀ phase was maintained even after the surface modification. The order-parameter *S* provides the

(7) (a) Baetzold, R. C. *Surf. Sci.* **1981**, *106*, 243. (b) Kodama, R. H.; Berokowitz, A. E.; McNiff, E. J.; Foner, S. *Phys. Rev. Lett.* **1996**, *77*, 394. (c) Bodker, F.; Morup, S.; Lideroth, S. *Phys. Rev. Lett.* **1994**, *72*, 282. (8) Kobayashi, T.; Seki, T. *Langmuir* **2003**, *19*, 9297. (9) Shimomura, M.; Kunitake, T. *J. Am. Chem. Soc.* **1982**, *104*, 1757. (10) Zhang, J.; Whitesell, J. K.; Fox, M. A. *Chem. Mater.* **2001**, *13*, 2323.

(11) Bagaria, H. G.; Ada, E. T.; Shamsuzzoha, M.; Nikles, D. E.; Johnson, D. T. *Langmuir* **2006**, *22*, 7732.

information about the degree of the structural transition, which can be defined as

$$S^2 = \frac{1 - S_a}{1 - S_f}$$

where S_a and S_f were a/c -axis ratios of the target samples and the perfectly ordered samples (known as 0.6939), respectively.¹² The S values for the as-prepared and composite states were the same value of 0.72 for both samples.

Transmission electron microscope (TEM) images of FePt nanoparticles both before and after surface modification and their size distribution are shown in Figure 2a–c, respectively. The ligand-coated FePt nanoparticles show good dispersibility and have a uniform nearest-neighbor spacing of 4.3 nm, while as-prepared “bare” particles tend to aggregate. This “neighbor spacing length” is in good agreement with the azo-ligand length of 4.1 nm calculated from the molecular model. This indicates the formation of a mixed monolayer of organic ligands on the surface of the FePt nanoparticles. The average diameter of the particles that appeared in the dispersion was 5.64 ± 1.35 nm.

We also investigated XPS measurements to confirm the existence of coordination bonds between the organic ligands and the surface atoms of the core particles in both the “as-prepared” and the composite states. XPS spectra were recorded at the characteristic photoenergies of Pt 4f in each state (Figure 3). Two components were found for Pt 4f in the composite state, while only one component was found in the as-prepared state. One component found in both states at a binding energy of 71.2 eV is the typical neutral state of Pt. Another component that appears at 72.3 eV, and which is only found in the composite state, is the nonzero charge state.¹³ The observation of the nonzero charge state indicates the existence of charged atoms due to coordination bonds with organic ligands. The relative contributions of both components to the spectra are ca. 80% for the neutral state and ca. 20% for the nonzero charge state, respectively. The relative proportion of ca. 20% for the nonzero charge state is very similar to the relative proportion of surface atoms to all atoms for an entire particle. Sun et al. also reported that amine and carboxylate ligands form good coordination bonds with FePt nanoparticles and that Fe tends to bind with $-\text{OOC}$, while Pt binds to NH_2 .¹⁴

Photoisomerization. The photoisomerization of composite FePt nanoparticles in the solid state at room temperature was monitored by UV–visible adsorption spectroscopy. Changes in the UV–vis spectra due to photoisomerization are shown in Figure 4. The spectrum of the initial state gave an intense absorption peak at 350 nm. This peak is ascribed to the $\pi-\pi^*$ transition in the trans-isomer of the azo-ligands. In this state, the composite FePt nanoparticles only consisted of the trans-isomer of the azo-ligands, because this is thermodynamically more stable than the cis-isomer¹⁵ (black line). After UV

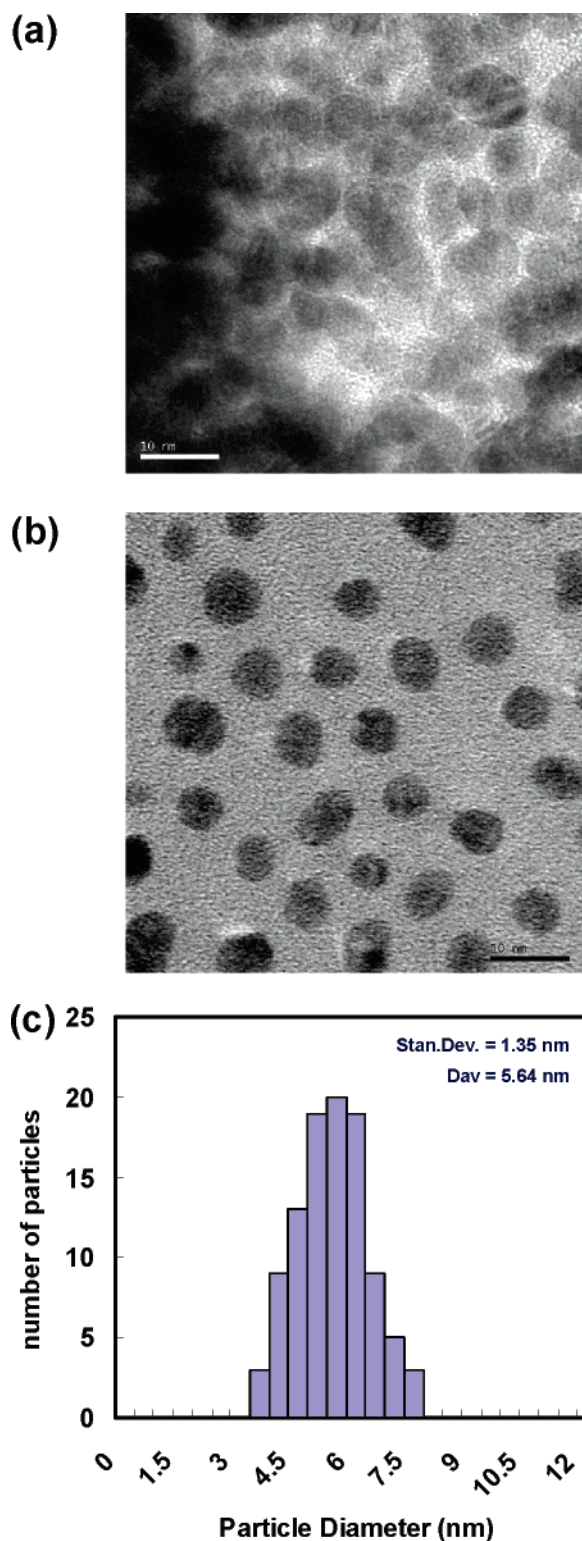


Figure 2. TEM micrograph of the FePt nanoparticles. (a) TEM micrograph of the as-prepared state; scale bar = 10 nm. (b) TEM micrograph of the composite state; scale bar = 10 nm. (c) The size distribution of the particles that appeared in the dispersion (in (b)) was 5.64 ± 1.35 nm.

illumination of the trans-isomer for 1 min, the absorption at 350 nm decreased (blue line). This indicates that trans-to-cis photoisomerization occurred in the composite FePt nanoparticles. Following subsequent illumination with visible light for 1 min, the absorption at 350 nm increased again (orange line), indicating that cis-to-trans photoisomerization also occurred.

(12) Roberts, B. W. *Acta Metallogr.* **1954**, *2*, 597.

(13) (a) Stahl, B.; Gajbhiye, N. S.; Wilde, G.; Kramer, D.; Ellrich, J.; Ghafari, M.; Hahn, H.; Gleiter, H.; Weissmüller, J.; Würschum, R.; Schlossmacher, P. *Adv. Mater.* **2002**, *14*, 1, 24. (b) Stahl, B.; Ellrich, J.; Teissmann, R.; Ghafari, M.; Bhattacharya, S.; Hahn, H.; Gajbhiye, N. S.; Kramer, D.; Viswanath, R. N.; Weissmüller, J.; Gleiter, H. *Phys. Rev. B* **2003**, *67*, 14422.

(14) Sun, S.; Anders, S.; Thomson, T.; Baglin, J. E. E.; Toney, M. F.; Hamann, H. F.; Murray, C. B.; Terris, B. D. *J. Phys. Chem. B* **2003**, *107*, 5419.

(15) Adamson, A. A.; Volger, A.; Kunkely, H.; Wachter, R. *J. Am. Chem. Soc.* **1978**, *100*, 1298.

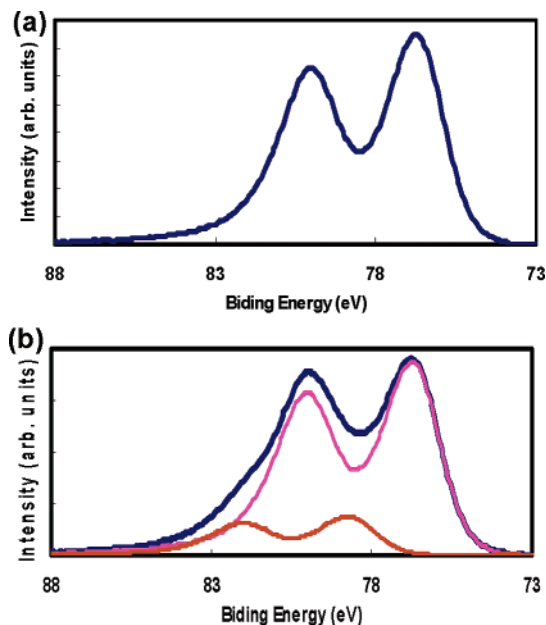


Figure 3. XPS analysis of the FePt nanoparticles. (a) XPS spectra of the Pt 4f edges for the as-prepared state; only one component was found at a binding energy of 71.2 eV (blue line), which is the typical neutral state of Pt. (b) XPS spectra of the Pt 4f edges for the composite state; another component was found at a binding energy of 72.3 eV (red line), which is the nonzero charge state of Pt.

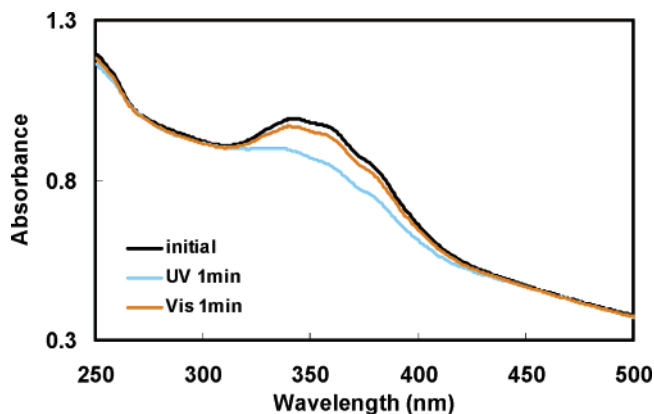


Figure 4. Changes in the optical adsorption spectra for the composite FePt nanoparticles due to the photoisomerization. The initial trans-state (black line) was first illuminated with UV light for 1 min (blue line). It was then illuminated with visible light for 1 min (orange line).

After the second cycle, cis–trans photoisomerization was repeated without any attenuation of the area between the curves (blue line to orange line). These reversible spectral changes indicate high-efficiency reversible photoisomerization, even in the solid state. Normally, the photoisomerization of azobenzene-containing compounds does not occur in the solid state, because photoisomerization is usually accompanied by a large change in volume.¹⁶ In this system, the presence of *n*-octylamine in the form of spacer ligands enables the reversible photoisomerization of the azo-ligands (even in solid state) because it provides sufficient free volume between the azo-ligands. Similar results have also been demonstrated in our previous works. To confirm this role of the spacer ligands, we designed other composite FePt nanoparticles that only consisted of azo-ligands by using alternative amine-modified azo-ligands such as compound **2**

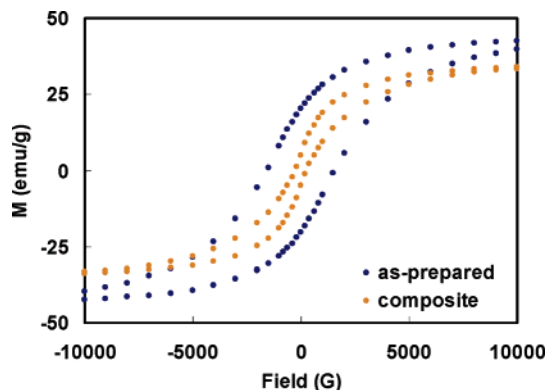


Figure 5. Magnetization curves of the FePt nanoparticles at 300 K. Plot of magnetization M versus applied magnetic field for the initial state (blue line) and the composite state (orange line).

instead of *n*-octylamine. Although trans-to-cis photoisomerization was observed in this system, the efficiency of the cis-to-trans photoisomerization was dramatically lower as compared to that of the other system. The outcome was that acceptable reversible photoisomerization in the solid state was only realized by using “spacer ligands” to guarantee sufficient free volume for photoisomerization to occur.

Photomagnetic Properties. The magnetic properties of the composite FePt nanoparticles were studied by SQUID measurements. The magnetization curves measured at 300 K before and after the surface modification are shown in Figure 5. In the as-prepared state, typical ferromagnetic behavior featuring a hysteresis loop with coercivity (H_c) and remanent magnetization (M_r) was observed at room temperature. The values of H_c and M_r were 1500 G and 20.3 emu/g, respectively. After the surface modification, the magnetization curve also showed ferromagnetic behavior, with H_c of 250 G and M_r of 4.38 emu/g, although the magnetic properties became inferior as compared to the as-prepared state. The reasons for this are thought to be the selective dispersion of small and platinum-rich particles^{6a} and surface charges due to coordination bonds with organic ligands.

Subsequently, we investigated the influence of photoillumination on the magnetic properties of the composite FePt nanoparticles at 300 K (Figure 6a). During the UV illumination, the initial magnetization value at 10 G increased from 3.13 to 3.44 emu/g. We then illuminated the composite FePt nanoparticles with visible light, and the magnetization value decreased from 3.44 to 3.21 emu/g. Even after the illumination was stopped, the increased magnetization value was maintained for at least 2 h. After this process, the UV light-induced increase and visible light-induced decrease in magnetization were repeated at least four times. The photoinduced changes in the magnetization values were estimated to be 9.9% in the first cycle and 7.3% after the second cycle. This decrease in the values after the second cycle is also consistent with the decrease in the efficiency of the photoisomerization after the second cycle.

We also examined the changes in the magnetization curves caused by photoillumination. Figure 6b shows the magnetization curves of the composite FePt nanoparticles in the initial and the UV illuminated states. After UV illumination, the hysteresis loop became slightly larger as compared to the initial state, with an increase in H_c from 250 to 300 G, and in M_r from 4.38 to 5.87 emu/g. That is, UV illumination caused the composite FePt nanoparticles to become slightly harder magnets.

(16) Nakahara, H.; Fukuda, K.; Shimomura, M.; Kunitake, T. *Nippon Kagaku Kaishi* **1988**, 7, 1001.

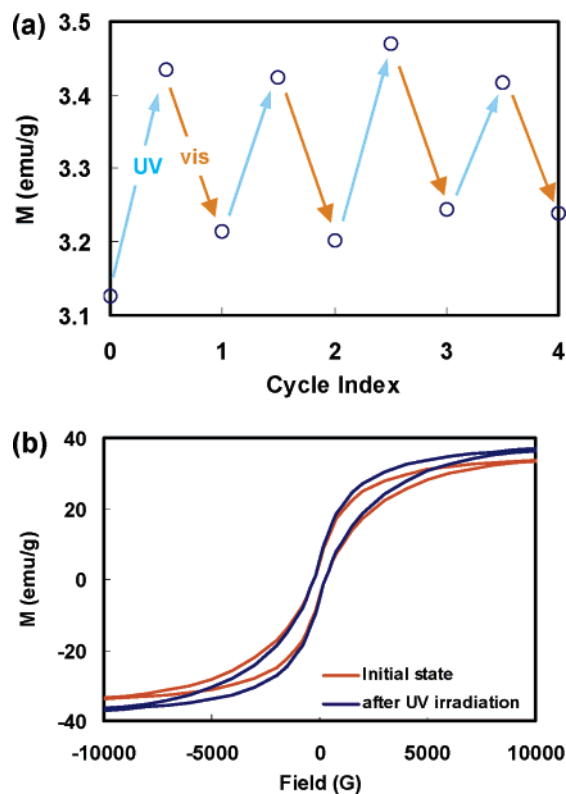


Figure 6. Photoinduced changes in the magnetic properties of the composite nanoparticles. (a) Changes in the magnetization. The composite nanoparticles were alternately illuminated with UV and visible light for 1 min each at 300 K with an external magnetic field of 10 G. (b) Changes in magnetization curves. Plot of magnetization M versus applied magnetic field before (orange line) and after (blue line) the UV illumination.

To confirm the effect of azo-ligands on the photoinduced changes in the magnetic properties, we also prepared a mixture of azo-ligands and FePt nanoparticles coated with long-chain alkyl “non-azo” ligands (prepared according to methods in the literature^{6a}). Although these samples showed magnetic properties very similar to those of the composite FePt nanoparticles, no changes in their magnetic properties were observed under UV or visible light illumination. These results suggest that the photoisomerization of azo-ligands, as well as the formation of coordination bonds with FePt nanoparticles, plays an important role in the photoinduced changes in the magnetic properties. This means that the photoinduced changes in magnetization were due to an interaction at the interfaces between the azo-ligands and the core particles, rather than the spatial relationship between each particle. Moreover, we have prepared the diluted sample, with the composite nanoparticles (coated with azo-ligands **1** and octylamine) being dispersed in PMMA matrix (see Supporting Information). The diluted sample clearly shows quite larger neighbor spacing length as compared to the pure samples. Therefore, it is expected that the possible magnetic interactions between each composite nanoparticles have been minimized in the diluted sample. Subsequently, we investigated the influence of photoillumination on the magnetic properties of the diluted sample. The UV light-induced increase and visible light-induced decrease in magnetization were also observed. Hence, it is concluded that not the changes in the magnetic interaction between each composite nanoparticle but the changes in the electronic interactions between the azo-ligands and the core-

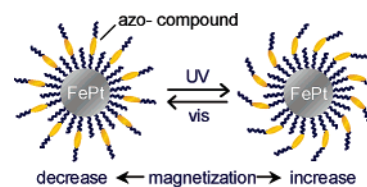


Figure 7. Schematic illustration of photoswitching of the magnetization of composite FePt nanoparticles.

FePt nanoparticles due to the photoisomerization were the origin of the photoinduced changes in the magnetic properties.

From the above observations, it is proposed that the photoisomerization of azo-ligands caused the changes in the electrostatic field around the FePt nanoparticles. As a result, changes in the magnetization were induced by electronic polarization on the surfaces of the FePt nanoparticles. Figure 7 shows a schematic illustration of the photoinduced changes in the magnetization. Our previous work also demonstrated similar interactions between organic photochromes and inorganic magnetic systems.³

Moreover, to discuss the interaction between the interfaces, we have designed another set of composite FePt nanoparticles coated by compound **3** and octanoic acid (spacer ligands). In this case, azobenzene-derivatized ligands with thiol terminations bond covalently with the platinum atoms on the surface, while octanoic acid groups with carboxyl terminations coordinate to the iron atoms on the surface.¹¹ Although the reversible photoisomerization of azo-ligands in the solid state was also observed in this system, no changes in their magnetic properties were observed under illumination with UV or visible light. This result suggests that the photoinduced changes in the magnetic properties of the FePt nanoparticles were caused by changes in the electronic states of the iron atoms on the surfaces of the nanoparticles.

To confirm the photoinduced changes in the electronic states of the iron atoms directly, the ⁵⁷Fe Mössbauer spectra of the composite nanoparticles were measured before and after the UV light illumination (Figure 8). Stahl et al. have discussed the electronic states of iron atoms on organic-ligand-coated FePt nanoparticles with reference to their Mössbauer spectra.¹² They elucidated that organic-ligand-coated FePt nanoparticles exhibit two magnetic phases: one is a hyperfine interaction in the bulk-like core, while the other is a dipolar surface layer due to dipolar charges on the organic ligands. As considered in their discussions, the ⁵⁷Fe Mössbauer spectra of the composite FePt nanoparticles in both the initial and the UV illuminated states were fitted with four magnetic components. The doublet components in both states (blue line) were assigned to superparamagnetic particles, which were small particles that fell below the superparamagnetic limit. After the UV illumination, this superparamagnetic doublet fraction decreased. This decrease in the superparamagnetic component clearly shows that some of the superparamagnetic particles became ferromagnetic in nature after the UV illumination. These photoinduced enhancements in the magnetic properties were also consistent with photoinduced increases in the coercivity and the remanent magnetization that were confirmed by SQUID measurements. The sextet components with hyperfine fields of ca. 32 T (light blue line) and ca. 30 T (green line) in both states were assigned to the disordered fcc phase and the ordered L1₀ phase of the bulk-like particle core, respectively, because these hyperfine

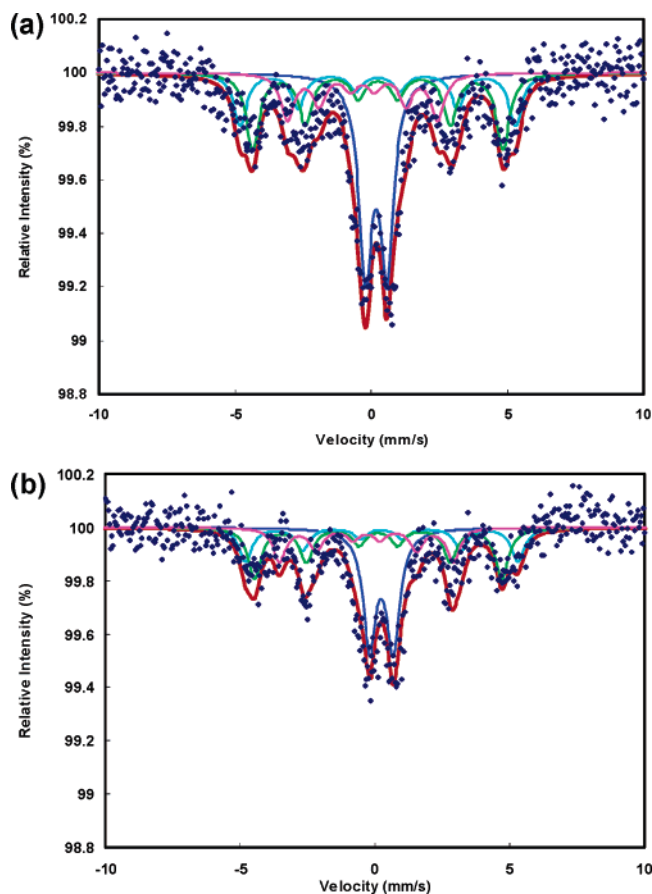


Figure 8. ^{57}Fe Mössbauer spectra for the composite nanoparticles at room temperature (a) before illumination and (b) after UV illumination.

parameters agreed with the reported values.¹⁷ No notable changes induced by photoillumination were observed in the Mössbauer parameters of these two phases, suggesting that no remarkable photoinduced changes in the magnetic properties had occurred in the bulk-like particle core. Moreover, another sextet component with a hyperfine field of ca. 18 T (pink line) was found in the initial state. We attributed this component to the surface Fe atoms on the core particles, which were electronically polarized by the dipolar charge of the organic ligands. These differences in magnetic phase between the particle cores and the particle surfaces form electronic shell structures with significant gradients in their electronic charge densities. After UV illumination, the hyperfine fields of the surface-layer phase changed from ca. 18.3 to ca. 21.4 T. These photoinduced changes in the hyperfine field mean that the photoisomerization of the azo-ligands had induced electronic polarization on the surfaces of the FePt nanoparticles. As a result, changes in the magnetic properties of the composite nanoparticles were caused by photoinduced changes in the electronic charge density on the surface iron atoms.

These explanations are also consistent with the effects of organic ligands on magnetic nanoparticles that have been reported before now.¹⁸ For example, Gedanken et al. reported that iron nanoparticles exhibit large variations in their magnetic

properties when various organic ligands are bonded to the surface iron atoms. They concluded that these differences could be explained by the organic ligands bonding to iron atoms via the d electrons of the iron, whereby the organic ligands interact strongly with the d electrons and cause a large splitting of the doubly and triply degenerate d levels. This affects the spin state and the magnetization values. This in turn suggests that exchange interactions between the spins of the iron atoms can affect the magnetization. Furthermore, Zhang et al. reported that the magnetic properties of the nanoparticles change according to the type of organic ligands that are present. These phenomena are caused by changes in the spin–orbital coupling and surface anisotropy of the nanoparticles that are induced by exchanging the ligands. The above discussions also suggest that photoinduced changes in the electronic polarization of the d electrons of the surface iron atoms affect the magnetic properties of the FePt nanoparticles. That is, our system realized “ligand exchange-like” behavior induced by photoillumination using photochromes without actually exchanging the ligands.

Conclusions

We have designed ferromagnetic FePt nanoparticles coated with mixed monolayers of azobenzene-derivatized ligands and spacer ligands. Subsequently, we have succeeded in controlling the magnetic properties of ferromagnetic nanoparticles by photoillumination in the solid state at room temperature. Our results suggest that these phenomena are due to changes in the electronic polarization on the d electrons of the surface iron atoms that are induced by the photoisomerization of azo-ligands. In addition, another important aspect of this work is the role of *n*-octylamine in forming the spacer ligands, thereby guaranteeing sufficient free volume between the azo-ligands to allow photoisomerization to occur. The advantage of this system as compared to our previous work is that we have now demonstrated room-temperature ferromagnetism, which is an absolute requirement for practicable magnetic recording media. Finally, this work has not only proposed a new strategy for developing photofunctional materials, but has also opened up great possibilities for practical applications in future optical magnetic recording systems.

Acknowledgment. This work was supported by a Grant-in-Aid for Scientific Research on Priority Areas (417), the 21st Century COE program “KEIO Life Conjugate Chemistry” from the Ministry of Education, Culture, Sports, Science, and Technology (MEXT) of the Japanese Government, and the New Energy and Industrial Technology Development Organization (NEDO).

Supporting Information Available: TEM images, powder XRD patterns, UV–visible absorption spectra, and magnetic or photomagnetic properties of the reference samples and diluted sample. This material is available free of charge via the Internet at <http://pubs.acs.org>.

JA0682374

(18) (a) Kataby, G.; Kolytyn, Y.; Ulman, A.; Ferner, I.; Gedanken, A. *Appl. Surf. Sci.* **2002**, *201*, 191. (b) Vestsal, C. R.; Zhang, Z. *J. Am. Chem. Soc.* **2003**, *125*, 9828.

(17) Goto, T.; Utsugi, H.; Watanabe, K. *J. Alloys Compd.* **1994**, *204*, 173.